Aqueous chemical bleaching of 4-nitrophenol brown carbon by hydroxyl radicals; products, mechanism, and light absorption

Bartłomiej Witkowski[1]*, Priyanka Jain[1], Tomasz Gierczak[1]

[1]University of Warsaw, Faculty of Chemistry, al. Żwirki i Wigury 101, 02-089 Warsaw, Poland

5 *Correspondence to:* Bartłomiej Witkowski (bwitk@chem.uw.edu.pl)

Abstract. The reaction of hydroxyl radicals (OH) with 4-nitrophenol (4NP) in an aqueous solution was investigated at pH=2 and 9. The molar yield of the phenolic products quantified was ca. 0.2 at pH=2 and 0.4 at pH=9. The yield of 4-nitrocatechol (4NC) was higher at pH=9. At the same time, a lower number of phenolic products was observed at pH=9 due to irreversible reactions of some phenols formed when the pH>7. Mineralization investigated with a total organic carbon (TOC) analyzer

10 showed that after 4NP was completely consumed, approximately 85% of the organic carbon remained in the aqueous solution. Moreover, as inferred from the TOC measurements and the molar yields of the phenols formed, 65% of the organic carbon that remained in the aqueous solution was attributed to the non-aromatic products. The light absorption of the reaction solution between 250 and 600 nm decreased as a result of the OH reaction with 4NP. However, the 4NP solution showed a noticeable resistance to the chemical bleaching reaction investigated due to the formation of light-absorbing by-products. This

15 phenomenon effectively prolongs the time scales of the chemical bleaching of 4NP by OH by a factor of 3–1.5 at pH 2 and 9, respectively. The experimental data acquired indicated that both photolysis and the reaction with OH can be important processes for the removal of light-absorbing organic compounds from cloud water particles containing 4NP.

1 Introduction

Atmospheric brown carbon (BrC) is a subfraction of organic aerosols (OA) characterized by strong, wavelength-dependent absorption of electromagnetic irradiation near-ultraviolet (UV) and visible (Vis) regions (Laskin et al., 2015; Yan et al., 2018). BrC is primarily produced by biomass burning (BB) and has a negative impact on local air quality and human health (Laskin et al., 2015; Hems et al., 2021). Due to the high UV-Vis absorption, BrC greatly contributes (up to 50%) to the radiative forcing of OA (Feng et al., 2013; Wang et al., 2014; Lu et al., 2015; Cordell et al., 2016; Zhang et al., 2017; Yan et al., 2018). Numerous organic compounds contribute to atmospheric BrC (Laskin et al., 2015; Li et al., 2020; Fleming et al., 2020; Vidović et al., 2020; Hettiyadura et al., 2021). At the same time, a significant fraction of BrC chromophores remains poorly characterized (Laskin et al., 2015; Bluvshtein et al., 2017).

Nitrophenols are widespread nitroaromatic compounds that have been identified among the major chromophores of atmospheric BrC (Harrison et al., 2005b; Kitanovski et al., 2012; Claeys et al., 2012; Laskin et al., 2015; Frka et al., 2016; Bluvshtein et al., 2017). 4-Nitrophenol (4NP) is one of the most atmospherically abundant and environmentally widespread nitrophenols (Harrison et al., 2005b; Laskin et al., 2015). 4NP also exhibits a strong absorption of electromagnetic radiation in the UV-Vis region (Jacobson, 1999). For these reasons, 4NP was found to contribute significantly to the light absorption of ambient BrC aerosols (Mohr et al., 2013; Bluvshtein et al., 2017; Kitanovski et al., 2020). 4NP was detected in the air, rain, surface waters, and snow as well as in atmospheric particulate matter (PM) (Jaber et al., 2007; Kitanovski et al., 2012; Claeys et al., 2012; Kahnt et al., 2013; Mohr et al., 2013; Balasubramanian et al., 2019; Liang et al., 2020; Kitanovski et al., 2020). Large quantities of 4NP are produced by the combustion of fossil fuels and biomass (Desyaterik et al., 2013; Mohr et al., 2013; Inomata et al., 2015; Xie et al., 2019). Moreover, 4NP is introduced into the environment by industrial processes (Majewska et al., 2021). Several studies have confirmed that 4NP has an adverse impact on human health (Majewska et al., 2021), is a threat to aquatic organisms (Tenbrook et al., 2003), and contributes to the decline of forests (Natangelo et al., 1999).

The formation, chemical processing, and removal (bleaching) of BrC can occur in the air as well as in atmospheric aqueous particles, and can involve direct photolysis and reactions with hydroxyl radicals (OH) (Laskin et al., 2015; Forrister et al., 2015; Moise et al., 2015; Hems and Abbatt, 2018; Hems et al., 2020; Li et al., 2020; Jiang et al., 2021). Due to the high value of Henry's law constant (Sander, 2015), and its high solubility in water, 4NP can readily partition into atmospheric aqueous particles (Harrison et al., 2005b; Vione et al., 2009). The chemical and photochemical reactions in the atmospheric aqueous phase contribute to the formation (Vione et al., 2003; Harrison et al., 2005a; Heal et al., 2007), transformation (Vione et al., 2005; Vione et al., 2009), and removal (Harrison et al., 2005a; Braman et al., 2020) of 4NP. The chemical and photochemical processing (aging) in the aqueous phase results in a change in the light absorption of aqueous particles containing 4NP (Zhang et al., 2003; Zhao et al., 2015; Braman et al., 2020). However, the connection between the light absorbance and chemical composition of the aqueous 4NP solution that has been subjected to photolysis and oxidation by OH is poorly characterized (Zhang et al., 2003; Zhao et al., 2015).

50 The aqueous reaction of 4NP with OH (reaction I) is known to produce aromatic products, including hydroquinone (HH), 1,2,4-trihydroxylbenzene (1,2,4-THB), 4-nitrocatechol (4NC), and 4-nitropyrogallol (4NPG) (Tauber et al., 2000; Oturan et al., 2000; Zhang et al., 2003; Daneshvar et al., 2007; Biswal et al., 2013).

$$4NP + OH \rightarrow products \qquad (I)$$
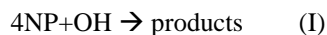
However, the yields of the substituted phenols from the reaction (I) remain ambiguous (Tauber et al., 2000; Oturan et al., 2000;
55 Zhang et al., 2003; Daneshvar et al., 2007; Ding et al., 2016). Reaction (I) was previously investigated at a molecular level but almost exclusively in the context of wastewater treatment via advanced oxidation processes (AOP) (Tauber et al., 2000; Oturan et al., 2000; Zhang et al., 2003; Ding et al., 2016) where the reaction conditions cannot be considered as atmospherically-relevant (Tauber et al., 2000; Zhang et al., 2003; Daneshvar et al., 2007; Ding et al., 2016). Consequently, it is currently difficult to evaluate if reaction (I) is a relevant source of atmospheric BrC (Oturan et al., 2000; Tauber et al., 2000; Kavitha
60 and Palanivelu, 2005; Biswal et al., 2013; Xiong et al., 2015).

In some clouds and fogs (Herrmann et al., 2015), 4NP (pKa≈7.2) (Rived et al., 1998) can exist in the protonated and deprotonated form (Fig. S1). At the same time, little information is available about the impact of pH on the distribution of the products of the reaction (I) (Tauber et al., 2000; Oturan et al., 2000). Furthermore, little information exists regarding the pH dependence of the light absorbance of a 4NP solution that has been subjected to OH oxidation (Biswal et al., 2013; Zhao et
65 al., 2015). It should also be noted that the UV-Vis absorption of 4NP and its aromatic oxidation products are strongly pH-dependent (Biswal et al., 2013; Braman et al., 2020).

The objective of this study was to investigate the mechanism of OH reactions with 4NP in the aqueous phase in the context of atmospheric BrC formation and processing. Therefore, reaction (I) was investigated at 298 K in an aqueous solution under acidic (pH=2) and basic (pH=9) conditions using the photoreactor developed in the host laboratory (Witkowski et al., 2019).
70 Additionally, the phenolic products of the reaction (I) were analyzed together with the changes in the UV-Vis absorption of the reaction solution. The phenols under investigation were quantified using gas chromatography coupled to mass spectrometry (GC/MS). The possible mineralization of 4NP and the formation of volatile products were monitored with a total organic carbon (TOC) analyzer. The UV-Vis absorption of the reaction solution, as well as the molar absorption (ε, $mol^{-1} \times L \times cm^{-3}$) of the phenols under investigation, were measured between pH 2 and 9.

75 **2. Experimental section**

The materials and reagents used are listed in section S1 of the electronic supplementary information (SI). All solutions were prepared using deionized (DI) water (18 M$\Omega \times cm^{-1}$).

2.1 Aqueous phase photoreactor

The aqueous photoreactor was described previously (Witkowski et al., 2019); more details are provided in section S4.1. The
80 reaction vessel was a quartz jacketed flask with an internal volume of 100 ml, surrounded by eight 4W lamps. All experiments

were carried out at 298 K; the temperature of the reaction solution was maintained by a circulating water bath (SC100-A10, Thermo Fisher Scientific). Two 4W lamps (TUV, peak emission 254 nm) and six 4W lamps (33-640, emission >400 nm, Philips) were used to irradiate the reaction solution.

2.2 Experimental procedure

85 The reaction mixture was a 100–250 µM aqueous solution of 4NP; total volume 100 ml. The pH of this solution was not adjusted (unbuffered, no acids or buffers added) or it was adjusted to pH 2 or 9 with HCl, HClO$_4$, or Na$_2$HPO$_4$ (50 mM) to investigate the reaction of fully protonated and deprotonated forms of 4NP (Fig. S1). Hydrogen peroxide (H$_2$O$_2$, concentration 5 mM) was photolyzed with UV irradiation (254 nm) to generate OH with an estimated steady-state concentration = 1.4×10^{-9} M (section S3) (Tan et al., 2009). Under these conditions, 4NP was almost completely consumed within 1h. Aliquots of the
90 reaction mixture were sampled every 5 min and analyzed with GC/MS, a UV-Vis spectrophotometer, and, a TOC analyzer. The experimental procedure is described in detail in section S4.1.

2.3 Quantification of the phenolic products with gas chromatography coupled to mass spectrometry

Analyses were carried out using a GC-MS-QP2010Ultra gas chromatograph coupled with a single quadrupole mass spectrometer and equipped with an AOC-5000 autosampler (Shimadzu). Analytes were separated using a capillary column
95 ZB-5MSPlus (Phenomenex). The mass spectrometer was equipped with an electron ionization source (EI, 70 eV) and was operating in the selected ion monitoring (SIM) mode. The instrument was calibrated with the standard solutions of 4NP, HH, 1,2,4-THB, and 4NC that were identified as products of the reaction (I). 2-Nitrophloroglucinol was used as a surrogate standard for the quantification of 4-nitropyrogallol (4NPG) and 5-nitropyrogallol (5NPG), both identified among the products of the reaction (I). Because phloroglucinol was not identified as the product of reaction (I) (Zhao et al., 2013; Xiong et al., 2015), it
100 was used as an internal standard (IS). The phenols were derivatized with acetic anhydride (AA) and analyzed with GC/MS (Regueiro et al., 2009). A detailed description of the analytical procedure is provided in section S4.2.

The yields of the phenols formed from reaction (I) were derived using eq. (I).

$$[Product]_t = Yield \times \Delta[4NP]_t \ (I)$$

In eq. (I), [Product]$_t$ is the concentration (or the sum of the concentrations) of the products at a given time (t) from the onset
105 of the reaction (mM). [4NP] is the amount of the precursor that reacted at a given time (t) from the onset of the reaction (mM) (Gierczak et al., 2021). Additionally, modeled yields of 4NC were derived with a kinetic box model (section S5).

2.4 UV-Vis spectrophotometry

UV-Vis measurements were performed with an i8 dual-beam spectrophotometer (Envisense) in 4 ml cuvettes with a 1 cm absorption pathlength; the spectral range was 230 to 600 nm. The absorbance of the aliquots of the reaction solution was
110 initially measured at pH=2 or 9, which was the pH of the reaction mixture (section 2.2). Subsequently, a small amount of

NaOH or H_3PO_3 was added to each sample taken from the reactor, the pH was adjusted by 1 unit and the absorbance was measured again. This procedure was repeated until the absorbance of each aliquot of the reaction solution was recorded between pH 2 and 9 (section S4.3). Separately, the wavelength-dependent absorption cross-sections, ε, $(mol^{-1} \times L \times cm^{-1})$ were measured (Fig. S6) for 4NP, HH, 1,2,4-BT, 4NC, and 2-NPG using the commercially available standards and are listed in Appendix 1.

2.5 Total organic carbon analyses

Non-purgeable organic carbon (NPOC) was quantified with a TOC-5050A analyzer (Shimadzu) equipped with an ASI-5000A autosampler (Shimadzu). The 1.5 ml of the reaction solution was diluted with the same volume of water, filtered through a 0.22 µm PTFE membrane, and placed in the TOC autosampler vial. Then, 50 µl of 2M HCl was added by the autosampler and each sample was purged with O_2 for 2 min before being injected to remove the CO_2 and the sparingly soluble, volatile organic compounds. The injection volume was ca. 20 µl and each sample was injected into the instrument three times. The TOC analyzer was calibrated with the standard solutions of 4NP (section S4.4).

2.6 Light absorption and atmospheric lifetimes

The production of light-absorbing compounds following reaction (I) was evaluated using eq. (II).

$$\frac{\left(\int_{250nm}^{600nm} A_{10}^{R.mix}(pH)\right)_t d\lambda}{\left(\int_{250nm}^{600nm} A_{10}^{4NP}(pH)\right)_t d\lambda} = \left(\frac{[4-NP]_0}{[4-NP]_t}\right)^{K_{abs}} (II)$$

In eq. (II), $A_{10}^{R.mix}$ and A_{10}^{4NP} are integrated absorbance peak areas between 250 and 600 nm (dλ) for the reaction mixture measured between pH 2 and 9 at different time intervals (t), $[4NP]_0$ and $[4NP]_t$ are the initial (0) and intermediate (t) concentrations of 4NP measured with GC/MS, and the absorbance (A_{4NP}) of 4NP was calculated by the Beer-Lambert law using the ε measured in this study between pH 2 and 9. The expression described by eq. (II) followed function $y = A \times x^K$ (section S9 and Fig. S11).

The atmospheric lifetime of BrC was evaluated by calculating the empirical $k_{bleaching}$ rate constant $(M^{-1}s^{-1})$ – eq. (III).

$$k_{bleaching=} k_{OH}(4-NP) \times \frac{k_{A.rmix}}{k_{A.4-NP}} (III)$$

In eq. (III), k_{OH} is the second-order rate constant $(M^{-1}s^{-1})$ for the reaction of 4NP or 4-nitrophenolate (4NPT) with OH (García Einschlag et al., 2003; Biswal et al., 2013), k_A and $k_{A.rmix}$ are the first-order disappearance rate constants (min^{-1}) of the integrated absorbance peak for the 4NP and the reaction mixture, respectively (Fig. S10). The $k_{A.rmix}$ values derived showed little dependence on the pH at which the absorbance was measured, thus average values were used.

The TOC-normalized mass absorption coefficients (MAC_{TOC}) of the reaction mixture were calculated using eq. (IV) (Laskin et al., 2015; Bluvshtein et al., 2017; Jiang et al., 2021).

$$MAC_{TOC}(\text{cm}^2 \times g_{TOC}^{-1}) = \frac{\ln(10)\left(\int_{250nm}^{600nm} A_{10}^{R.mix} \times l_{solution}^{-1}\right)_t d\lambda}{NPOC} \times 10^{-6} \text{ (IV)}$$

In eq. (IV), l is the optical path length (cm^{-1}), NPOC is the concentration of non-purgeable organic carbon (mg $\times$ L^{-1}). The TOC-normalized rate of sunlight absorption (R_{abs}) by the reaction solution was estimated using eq. (V) (Jiang et al., 2021).

$$R_{abs}(\text{photons} \times s^{-1} \times mg_{TOC}^{-1}) = \left(\frac{\ln(10) \times \left(\int_{250nm}^{600nm} A_{10}^{R.mix} \times l_{solution}^{-1} \times I_\lambda\right) d\lambda}{NPOC}\right) \times 10^{-3} \text{ (V)}$$

In eq. (V), I_λ is the actinic flux (photons$\times$ s$^{-1}\times$ cm$^{-2}\times$nm^{-1}) estimated by the TUV calculator for zenith angles 0-50° (Ncar, 2016).

2.7 Control experiments and uncertainty

The stability of the phenols under investigation in the presence of H_2O_2 or UV-Vis irradiation alone was studied in control experiments (section S7). Also, for the experiments at pH=2, HCl or HClO$_4$ was used to confirm that the buffering agent used did not affect the distribution of the detected products. The control experiments revealed that all the phenols under investigation were stable at pH≤7, within the time-scale of the experiments, but 1,2,4-THB, 4NPG, 5NPG, and HH underwent irreversible dark reactions at pH>7.

Experimental uncertainties are reported as 2σ from triplicate measurements, other uncertainties were calculated with the exact differential method unless otherwise noted.

3. Results and discussion

3.1 Products and reaction mechanism

The products of the reaction (I) formed under acidic pH conditions are shown in Fig. 1.
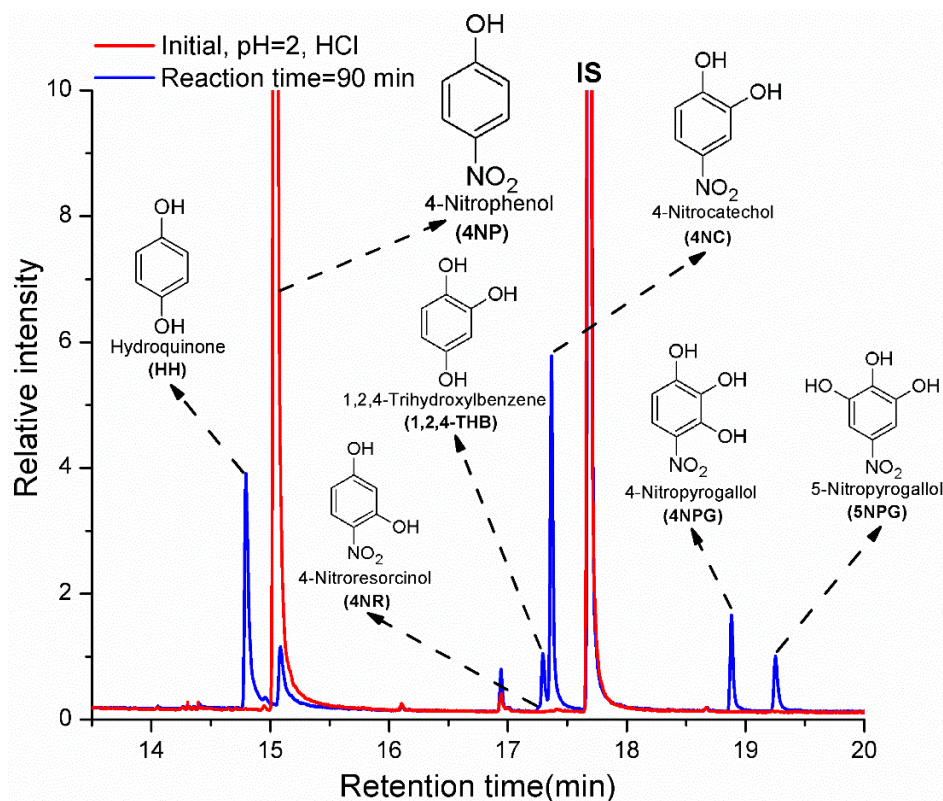
Figure 1: GC/MS chromatogram illustrating the formation of phenols from reaction (I) at pH=2.

HH, 1,2,4-THB, 4NC and 5NPG were formed from reaction (I) under acidic pH conditions (Fig.1), which is in good agreement with the previously published results (Oturan et al., 2000; Tauber et al., 2000; Liu et al., 2010; Xiong et al., 2015; Du et al., 2017; Chen et al., 2018). Previously, two unknown isomers of 4NC were detected as products of the reaction (I) (Zhao et al., 2013). Here, 4-nitroresorcinol (4NR), a structural isomer of 4NC, was also tentatively identified among the products for the first time. Moreover, this study is the first to report the formation of 4NPG from reaction (I) (Xiong et al., 2015). Previously, the formation of these two products (4NR and 4NPG) might have been difficult to observe due to the lack of standards and the absence of an MS detector (Tauber et al., 2000; Daneshvar et al., 2007; Liu et al., 2010). Furthermore, the insufficient resolving power of the HPLC used to study the products of the reaction (I) likely contributed to the fact that the formation of 4NR and 4NPG was not previously reported (Lipczynska-Kochany, 1991; Oturan et al., 2000; Tauber et al., 2000; Daneshvar et al., 2007; Liu et al., 2010).

The phenolic products of the reaction (I) were quantified with GC/MS; the results are presented in Fig. 2.
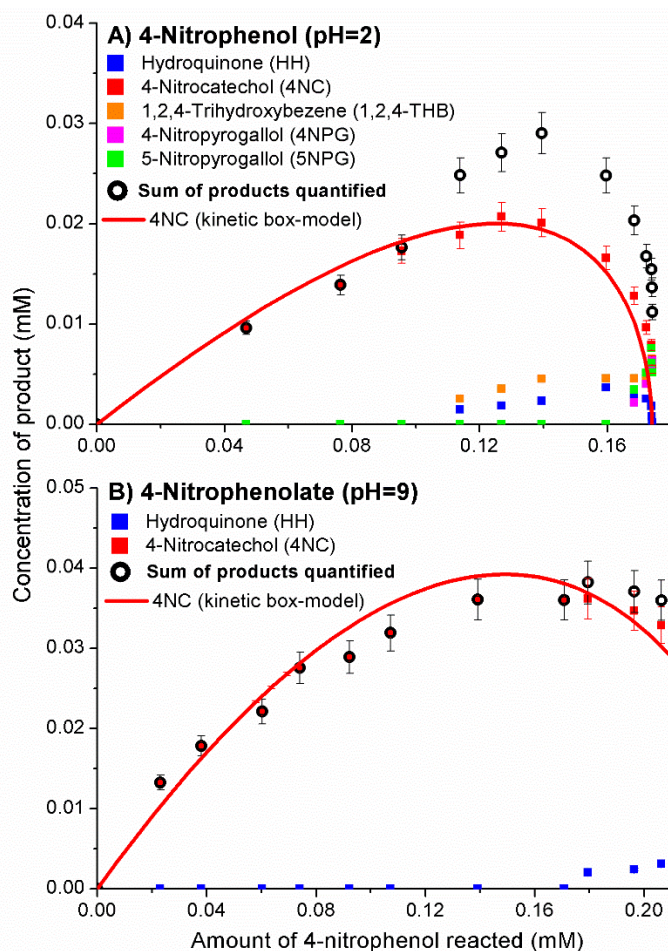
Figure 2: The formation of phenolic products from the 4-nitrophenol (A, pH=2) and 4-nitrophenolate (B, pH=9) + OH reaction. The molar yields for 4NC were estimated from the initial sections of the plots via linear regression analysis (Fig. S4 and Table S2). Plots derived with eq. (I) for the products quantified are expected to curve during the course of the reaction because these molecules are also reactive towards OH. The lines for 4NC are results of kinetic modeling (Table S3 and Fig. S5).

4NC was the major product of the reaction (I) under acidic and basic conditions. The second-generation products were HH, 1,2,4-THB, 4NPG, and, 5NPG (Fig. 2). The molar yields for 4NC, obtained as slopes of the initial sections of the plots shown in Fig. 2, were ca. 0.2 at pH=2 and ca. 0.4 at pH=9 (Fig. S4).

A kinetic box-model was constructed to provide more insights into the mechanism of reaction (I). The expected curving of the plots in Fig. 2A is likely due to the reaction of 4NC with the OH (Gierczak et al., 2021). However, for the reaction of 4NPT (pH=9), the results of kinetic modeling indicate regeneration of 4NC from 4NC+OH reaction with a yield of 0.5 (Table S3) (Tauber et al., 2000; Di Paola et al., 2003). Under these assumptions, the modeling results correlated well with the experimental data acquired (Fig. 2 and S5).

The results of the experiments carried out in pure water (no acids or buffers added) are not included in Fig. 2. The pH of the unbuffered reaction solution quickly decreased to ca. 3.5 (Di Paola et al., 2003), likely due to the formation of nitrite (NO_2^-) and nitrate (NO_3^-) (Kotronarou et al., 1991; Lipczynska-Kochany, 1991; Kavitha and Palanivelu, 2005; Liu et al., 2010). For this reason, the distribution of products in the acidic reaction solution and a pure water was the same.

The proposed mechanism of reaction (I) is presented in Fig. 3.
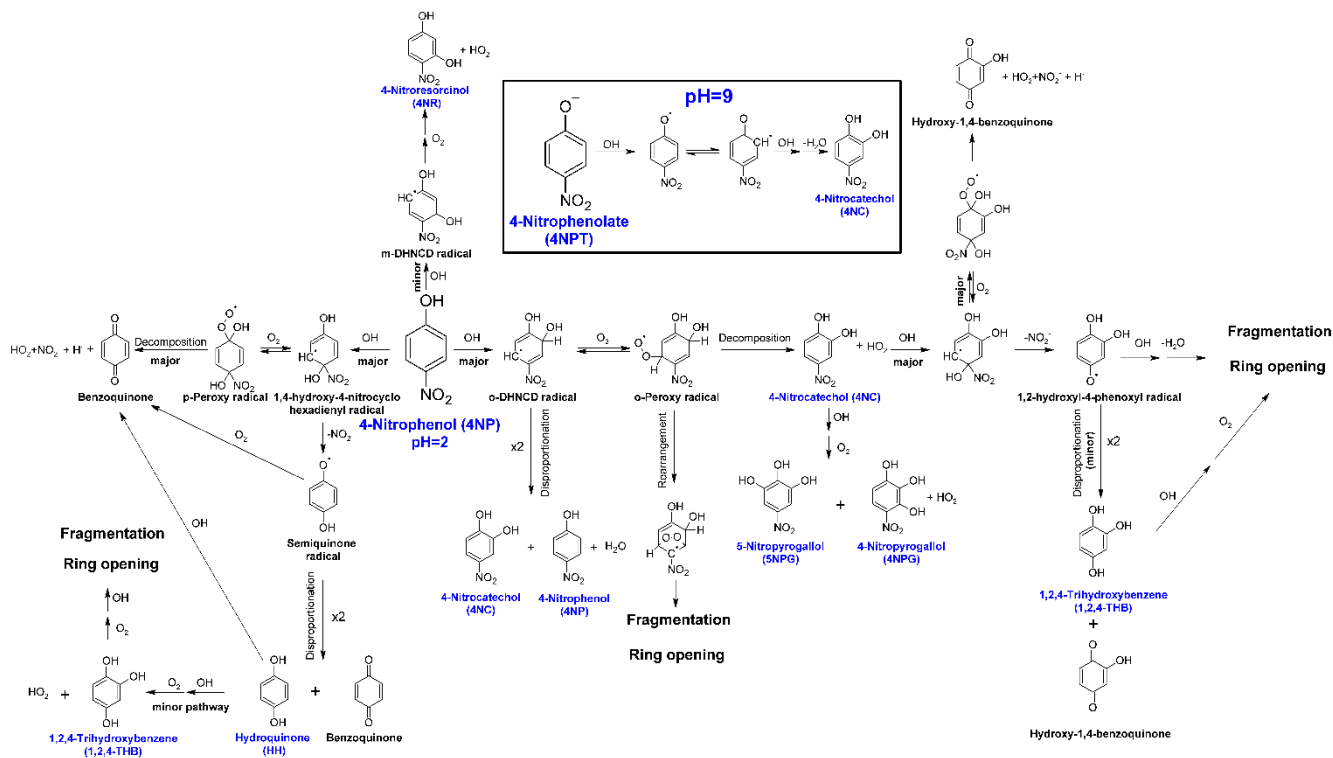
Figure 3: The proposed mechanism for the reaction of OH with 4-nitrophenol in an aqueous solution. The names of the compounds detected with GC/MS are shown in blue. All possible fragmentation and reaction pathways of the radical by-products are not included, for clarity.

Reaction (I) is initiated by the electrophilic addition of OH, primarily in the ortho and para positions of 4NP, yielding dihydroxynitrocyclohexadienyl (DHNCD) radicals – Fig. 3 (Kotronarou et al., 1991; Di Paola et al., 2003; Kavitha and Palanivelu, 2005). Two ortho-DHNCD radicals can then disproportionate to form 4NC and regenerate 4NP (Tauber et al., 2000; Gonzalez et al., 2004; Liu et al., 2010; Zhao et al., 2013). Alternatively, 4NC is formed by the reaction of o-DHNCD with O_2 and decomposition of the resulting o-peroxy radical (Oturan et al., 2000; Di Paola et al., 2003; Liu et al., 2010; Xiong et al., 2015; Ding et al., 2016). Due to the lower molar yield of phenols at pH=2 (0.2), the ortho-addition primarily yields ring-opening products. The addition of OH at the meta position of 4NP (minor pathway) leads to the formation of 4-NR (Fig. 1). Likewise, 4NPG and 5NPG (second-generation products) are most likely formed following the 4NC+OH reaction, which also involves the formation of a peroxy-type radical.

200 Moreover, only trace amounts of 1,2,4-THB were formed from 4NC+OH under acidic conditions (section S8 and Fig. S7) (Oturan et al., 2000; Zhang et al., 2003; Xiong et al., 2015; Ding et al., 2016; Du et al., 2017). As previously reported, 4NC was quantitatively converted into 1,2,4-THB in the absence of O_2, which promotes the disproportionation reaction between the two 1,2-hydroxyl-4-phenoxyl radicals formed by the ipso addition of OH to 4NC (Di Paola et al., 2003; Gonzalez et al., 2004; Liu et al., 2010). Hence, at pH=2 and in the presence of O_2, the formation of 1,2,4-THB from the 4NC+OH following

205 the disproportionation reaction is a minor process (Fig. S7), which is consistent with the literature data (Liu et al., 2010). Consequently, it is proposed that 1,2,4-THB is likely formed following the ipso addition of OH to 4NP (Zhang et al., 2003; Kavitha and Palanivelu, 2005; Daneshvar et al., 2007). The resulting 1,4-hydroxy-4-nitrocyclohexadienyl (1,4-DH-4-NCD) type radical can then eliminate NO_2^- producing HH and 1,2,4-THB by the disproportionation mechanism (O'neill et al., 1978; Kotronarou et al., 1991). The formation of NO_2^- is also consistent with the observed rapid decrease in the pH of the unbuffered

210 reaction solution.

Previously, the formation of 1,2,4-THB from the HH+OH reaction was observed (Niessen et al., 1988; Barzaghi and Herrmann, 2002; Sobczyński et al., 2004). Therefore, under the experimental conditions used in this work, the low yield of HH is likely due to its rapid oxidation to 1,2,4-THB and BQ (not quantified) (Kotronarou et al., 1991; Oturan et al., 2000; Di Paola et al., 2003; Sobczyński et al., 2004; Gonzalez et al., 2004).

215 Due to the irreversible reactions of some phenols under investigation at pH=9 (Table S4), only 4NC and HH (a minor product) were detected as products of the reaction (I)– Fig. 2B. At the same time, the measured yield of 4NC increased from 0.2 (pH=2) to 0.4. At pH=9, reaction (I) can proceed by addition as well as by one-electron oxidation mechanisms- see the inset in Fig. 3 (Biswal et al., 2013; Zhao et al., 2013). The reactions of the 4-nitrophenolxyl radicals formed following the one-electron oxidation of 4NPT by OH are unclear (Gonzalez et al., 2004; Wojnárovits and Takács, 2008; Liu et al., 2010; Zhao et al.,

220 2013). It was proposed that such radicals can directly react with the OH, in the case of 4-nitrophenolxyl radicals such a reaction would yield 4NC (Niessen et al., 1988; Barzaghi and Herrmann, 2002). Moreover, as indicated by the results of kinetic modeling (section S5), 4NC may be regenerated from 4NC+OH reaction, which contributes to the higher measured yield (0.4) for this product from reaction (I) at pH=9. Consequently, the results obtained indicate that the deprotonation of 4NC and 4NP may enhance the disproportionation reaction of the nitrocyclohexadienyl-type radicals, which results in the regeneration of the

225 precursor (Niessen et al., 1988; Barzaghi and Herrmann, 2002).

3.2 Light absorption and the time-evolution of brown-carbon chromophores

The absorbance of the reaction solution decreased during the course of the reaction (section S9) for both 4NP and 4NPT. Previously, an initial small increase in the absorbance at 420 nm of the reaction 4NP solution (pH=5) was reported, followed by rapid bleaching (Zhao et al., 2015); these differences can be caused by the slightly different reaction conditions used. Also,

230 in this study, integrated absorbance values were used [eq. (II) and (III)] which may be a more adequate approach due to the shift of the maximum absorbance (A_{max}) of the reaction solution (Fig. S9) (Zhao et al., 2015; Hems and Abbatt, 2018).

The contribution of the light-absorbing products of the reaction (I) to the absorption of the reaction solution was evaluated with eq. (II) – the results are shown in Fig. 4.

235
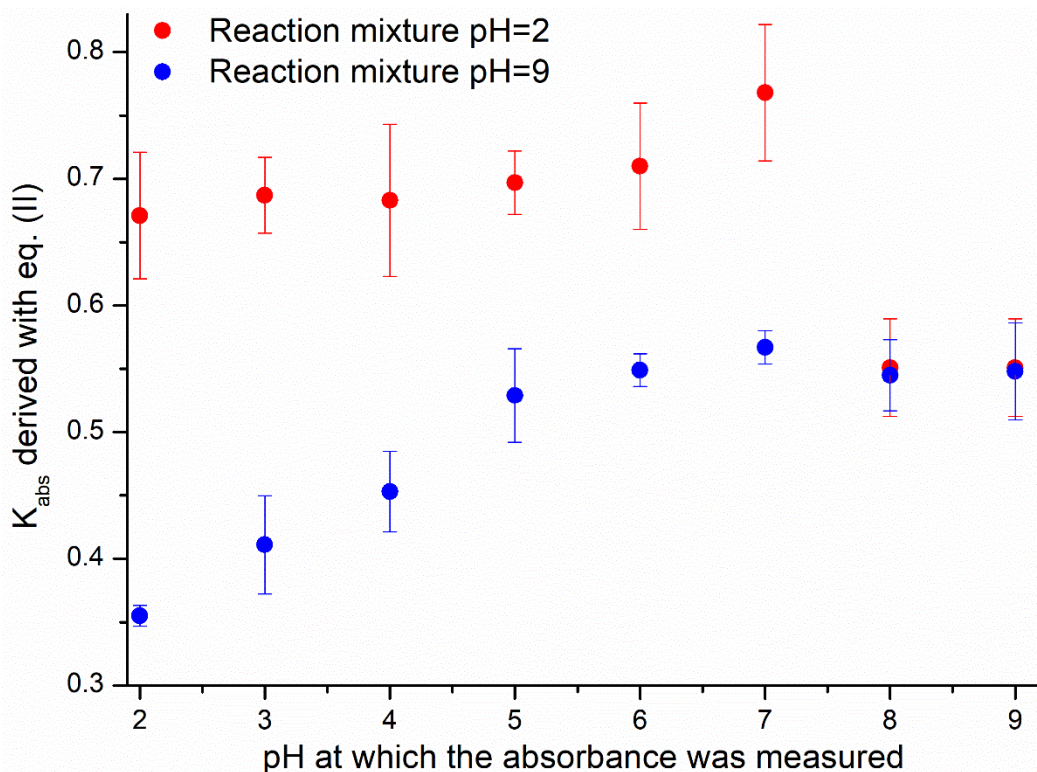
Figure 4: The ability of 4NP to generate products with an absorbance between 250 and 600 nm evaluated with K_{abs} factors derived using eq. (II). Uncertainties are precisions from the regression analysis.

240 The results presented in Fig.4 indicate that when the reaction was carried out under basic pH conditions the relative absorbance of the products was lower and increased more slowly. The absorbance of the products generated from 4NP (pH=2) decreased sharply when the pH of the solution before the UV-Vis measurement was adjusted to 8 and 9. Such a result indicates that the light-absorbing compounds are not stable at pH>7 which is in good agreement with the results presented in sections 3.1 and S6 (Randolph et al., 2018). The observed increase in the light absorption of the reaction solution (pH=9) between pH=2 and 9

245 could be due to the pH-dependence of the absorbance of the substituted carboxylic acids; aromatic ring-opening products (Oturan et al., 2000; Zhang et al., 2003; Kavitha and Palanivelu, 2005; Hems and Abbatt, 2018) with pK_a values likely falling between 3 and 6 (Rapf et al., 2017).

The values of MAC_{TOC} and R_{abs} calculated using eq. (IV) and (V) are presented in Fig. 5.
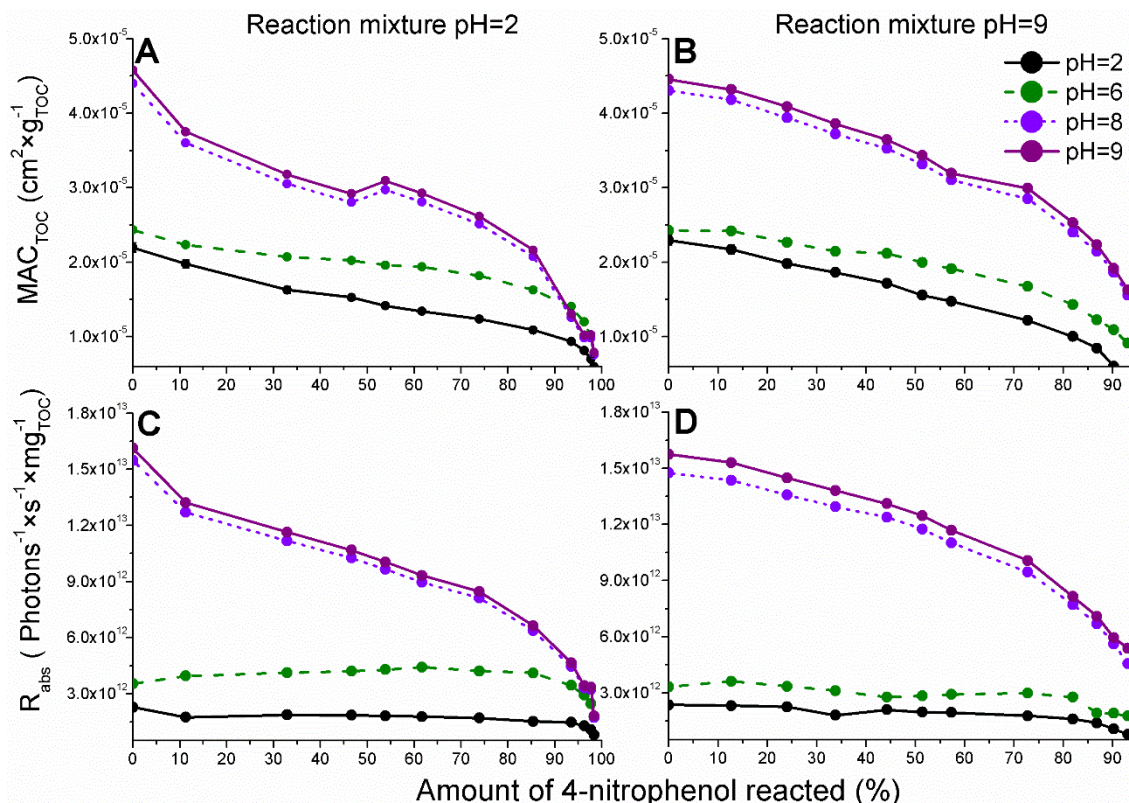
Figure 5: The pH-dependent organic carbon-normalized mass absorption coefficients (MAC$_{TOC}$) derived using the integrated absorbance peak for the reaction mixture absorption measured for the reaction of 4NP (A, pH=2) and 4NPT (B, pH=9) and the corresponding TOC-normalized rates of sunlight absorption (R$_{abs}$) for 4NP (C) and 4NPT (D). Only the data for pH =2, 6, 8, 9 are shown for clarity and the complete data are presented in Fig. S12. The colors refer to the pH at which the absorbance was measured (section 2.4). The experimental data are represented by points, with the lines provided to guide the eye.

As presented in Fig. 5, a decrease in the calculated MAC$_{TOC}$ was observed during the course of the reaction (I). Moreover, the experimental data acquired shows an increase of MAC$_{TOC}$ following the increase in pH at which the absorbance was measured (2, 6, 8, or 9). Such a result is likely due to the higher ε values for 4NP and 4NC under basic pH conditions (Fig. S6).

In Fig. 5A and 5B, the disappearance rate constants of MAC$_{TOC}$ are of a similar order. Such a result can be explained by the formation of a higher number of light-absorbing phenols (second-generation products) at pH=2 and also due to the higher formation yield of 4NC, which has high ε values at pH=9. Consequently, the disappearance rate constants of the overall light absorption of 4NC following reaction (I) are mostly independent of the pH of the reaction solution and primarily depend on the pH at which the absorbance is measured. The MAC$_{TOC}$ values calculated were slightly higher compared with the values measured for the previously investigated aromatic BrC chromophores (derived from the non-nitrated precursors) (Jiang et al., 2019; Jiang et al., 2021), likely due to the high ε values of 4NP and the nitrated phenols generated by the reaction (I).

The R$_{abs}$ values (Fig. 5C and 5D) decrease slower compared with the values of MAC$_{TOC}$ and become stable when the pH at which the absorbance was measured is less than 7 (see also Fig. S12). This is likely due to a red-shift of the A$_{max}$ of the reaction

solution, likely connected to the red-shift of the 4NP and 4NCs absorbance following the increase in the pH (Fig. S6). As presented in Fig. S14, the actinic flux exhibits a significant increase between 300 and 400 nm. Consequently, the BrC chromophores – products of the reaction (I) – characterized by a strong absorbance above 400 nm, will contribute to the observed stabilization of the estimated R_{abs} at pH<7.

3.3. Atmospheric implications

The average measured Henry's law constant – 5×10^4 ($M\times atm^{-1}$) – indicates that 4NP exists entirely in the aqueous phase in clouds but not in "wet" aerosols (Fig. S13) (Herrmann et al., 2015). Once dissolved in cloud water, 4NP can undergo chemical and photochemical processing; thus, the rates of the bleaching of the 4NP solution due to the reaction with OH were evaluated – Table 1.

Table 1. The pH-dependent second-order rate constants, empirical bleaching rate constants, and the effective quantum yields of photolysis were used to estimate the lifetimes of 4NPs and the corresponding BrC

Reactive species	$K_{A.4NP}$ (min^{-1})	$K_{A.rmix}$ (min^{-1})	$k_{OH} \times 10^{-9}$ (M^{-1}s^{-1})	Reference	$k_{bleaching} \times 10^{-9}$ (M^{-1}s^{-1}) (this work)	Lifetime of BrC relative to the lifetime of 4NP
				Reaction with OH		
			6.2	(Biswal et al., 2013)		
	0.047	0.016	4.1	(García Einschlag et	1.6	3
4NP			3.8	al., 2003)		
(pH<3)			4.7	Average literature		
				value		
4NPT	0.029	0.019	8.7	(Biswal et al., 2013)	6.0	1.5
(pH>8)						
				Photolysis		
Reactive species			φ (molecules $\times$ photon^{-1}) $\times 10^6$			Reference
4NP (pH<3)			110.0[a]			(Lemaire et al., 1985; Braman et al., 2020)

| 4NPT | 5.5 | (Lemaire et al., 1985) |
| (pH>8) | | |

[a]The average quantum yields measured in the presence of photorecalcitrant α-pinene SOA used as a scavenger of the secondary OH formed following the photolysis of HONO formed during the photolysis of 4NP.

280 Presented in Table 1, the first-order $k_{bleaching}$ rate constants were derived with eq. (II) using the experimental data acquired in this study and the lifetimes due to the reaction with OH were estimated with eq. (SIII). The data summarized in Table 1 shows that the lifetimes of BrC chromophores are 3 and 1.5-times longer than the lifetime of 4NP (precursor) under acidic and basic pH conditions, respectively, due to the formation of light-absorbing products.

The previously reported average quantum yields (ϕ, molecules×photon^{-1}) (Lemaire et al., 1985; García Einschlag et al., 2003;

285 Biswal et al., 2013; Braman et al., 2020) were used to derive the lifetimes of 4NP due to photolysis using eq. (SIV). The literature ϕ values listed in Table 1 were derived by measuring the decrease in the absorbance of the 4NP solution, hence can be regarded as effective ϕ for the bleaching of chromophores in aqueous solutions of 4NP and 4NPT (Lemaire et al., 1985; Braman et al., 2020). To our knowledge, the wavelength-dependent ϕ values for 4NP and 4NPT are not available. The estimated lifetimes of light-absorbing compounds in the cloud water particles containing 4NP due to direct photolysis and due

290 reaction with the OH were compared (Fig. 6).
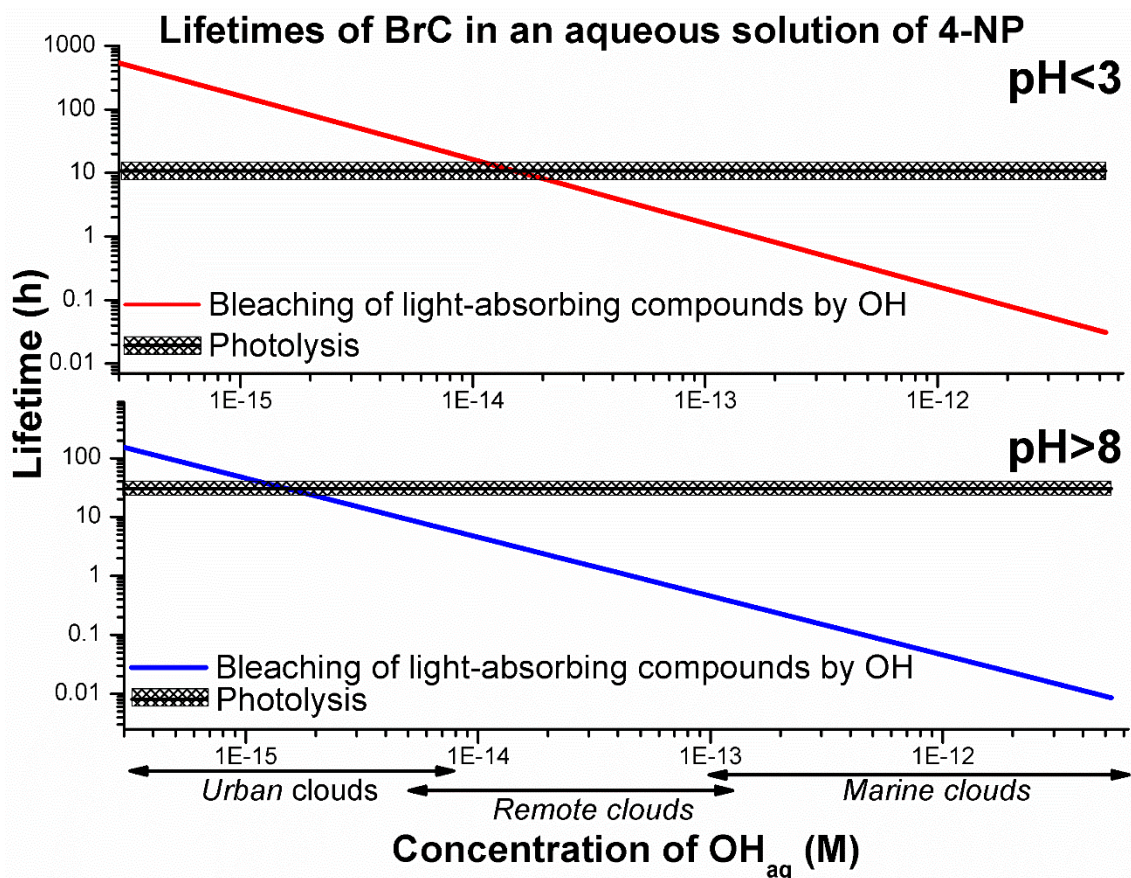
Figure 6: The estimated aqueous-phase lifetimes of light-absorbing compounds in solutions of 4NP and 4NPT. The lifetimes due to the reaction with OH were calculated with $k_{bleaching}$ rate constants derived with eq. (III) using the experimental data acquired in this study. The average lifetime due to photolysis is shown, shaded areas are 2σ values, representing the range of photolysis lifetimes calculated for the solar zenith angles 0–50°.

As presented in Fig. 6, the photolysis of 4NP BrC may be relevant under realistic atmospheric conditions in urban and remote clouds, with the estimated concentration of OH_{aq} lower than 1×10^{-13} M (Herrmann et al., 2010). Bleaching by OH is expected to be a more efficient removal mechanism for 4NPT, due to its lower reported quantum yields (ϕ) combined with the higher reactivity of the precursor towards OH at pH>8 (Lemaire et al., 1985; Braman et al., 2020).

A low degree of mineralization of the precursor (ca. 15%) was observed for both 4NP and 4NPT, as presented in Fig. 7.
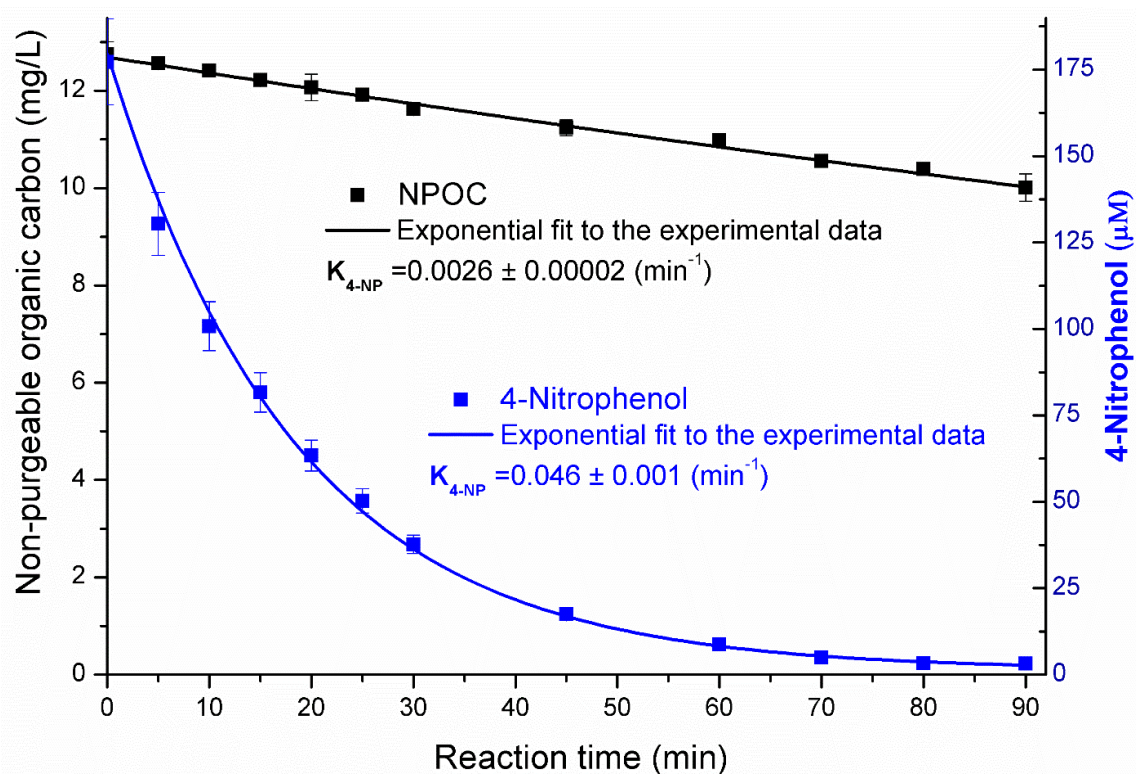
Figure 7: The concentrations of 4NP and non-purgeable organic carbon during the reaction in pure water. The results obtained for pH=2 and 9 reaction solutions were very similar – section S12. The uncertainties for the first-order decay rates (K, min[-1]) are standard errors from the regression analysis.

305 Due to the low degree of mineralization of 4NP (Fig. 7) combined with the yields of phenolic products calculated as ~0.2 (pH=2) and ~0.4 (pH=9), it is estimated that the yield of non-aromatic products from reaction (I) was between 0.45 and 0.68. These aromatic ring-opening products may include functionalized carboxylic acid, as previously proposed (Oturan et al., 2000; Zhang et al., 2003; Kavitha and Palanivelu, 2005; Hems and Abbatt, 2018).

4. Conclusions

310 The results acquired in this study show that the reaction of OH with 4NP in cloud water leads to the bleaching of light-absorbing compounds. Previously, the reaction with OH was concluded to be a major removal mechanism for several of nitrophenols in the atmospheric aqueous phase (Vione et al., 2009; Albinet et al., 2010; Zhao et al., 2015). As previously reported, the reaction of OH with 5-nitroguaiacol, 4NC, and dinitrophenol initially lead to a small increase in the light absorption followed by rapid bleaching (Zhao et al., 2015; Hems and Abbatt, 2018) but such behavior was not observed for 4NP in this study. By comparing

315 the results obtained in this study with the literature data (Zhao et al., 2015; Hems and Abbatt, 2018), it can also be concluded that more substituted nitrophenols initially yield higher amounts of light-absorbing products compared to 4NP. Moreover, the

atmospheric lifetimes of BrC chromophores due to the reaction with OH are expected to be significantly longer than the lifetimes of the parent nitrophenols (precursors) due to the formation of light-absorbing by-products (Zhao et al., 2015; Hems and Abbatt, 2018). The results obtained here and the data from the literature also indicate that the aqueous reaction of

320 nitrophenols with OH can potentially contribute to cloud water acidity due to the formation of NO_2^-, NO_3^- and organic nitro carboxylic acids (Tilgner et al., 2021). Additionally, the aqueous oxidation of nitrophenols by OH may be an important source of potentially toxic and harmful aqueous SOAs due to the formation of nitrogen-containing organic compounds combined with the low degree of mineralization of such precursors.

Data availability. The raw data can be obtained by contacting the corresponding author.

325 *Author contributions.* BW designed the study, developed the methodology, analyzed the data, and wrote the paper. PJ carried out the experiments, optimized the methodology, and processed the raw data. TG supervised the experiments, analyzed the data and contributed to the final manuscript. All authors contributed to the interpretation of the results.

Competing interests. The authors declare that they have no conflicts of interest

Acknowledgments. This work was carried out at the Biological and Chemical Research Centre, University of Warsaw,

330 established within the project co-financed by the European Union from the European Regional Development Fund under the

Operational Programme Innovative Economy, 2007–2013. We thank Dr. Bartłomiej Kiersztyn for making the TOC measurements possible. We thank the anonymous reviewers for the very insightful comments and suggestions.

Financial support. This project was funded by the Polish National Science Centre: grant number UMO-2018/31/B/ST10/01865. The authors also acknowledge the support from the statutory research funds of the University of
335 Warsaw, decision number BOB-661-199/2020.

References

Albinet, A., Minero, C., and Vione, D.: Phototransformation processes of 2,4-dinitrophenol, relevant to atmospheric water droplets, Chemosphere, 80, 753-758, https://doi.org/10.1016/j.chemosphere.2010.05.016, 2010.
Balasubramanian, P., Balamurugan, T. S. T., Chen, S.-M., and Chen, T.-W.: Simplistic synthesis of ultrafine $CoMnO_3$
340 nanosheets: An excellent electrocatalyst for highly sensitive detection of toxic 4-nitrophenol in environmental water samples, J. Hazard. Mater., 361, 123-133, https://doi.org/10.1016/j.jhazmat.2018.08.070, 2019.
Barzaghi, P. and Herrmann, H.: A mechanistic study of the oxidation of phenol by $OH/NO_2/NO_3$ in aqueous solution, Phys. Chem. Chem. Phys., 4, 3669-3675, 10.1039/B201652D, 2002.
Biswal, J., Paul, J., Naik, D. B., Sarkar, S. K., and Sabharwal, S.: Radiolytic degradation of 4-nitrophenol in aqueous
345 solutions: Pulse and steady state radiolysis study, Radiat. Phys. Chem., 85, 161-166, https://doi.org/10.1016/j.radphyschem.2013.01.003, 2013.
Bluvshtein, N., Lin, P., Flores, J. M., Segev, L., Mazar, Y., Tas, E., Snider, G., Weagle, C., Brown, S. S., Laskin, A., and Rudich, Y.: Broadband optical properties of biomass-burning aerosol and identification of brown carbon chromophores, J. Geophys. Res. Atmos. , 122, 5441-5456, https://doi.org/10.1002/2016JD026230, 2017.
350 Braman, T., Dolvin, L., Thrasher, C., Yu, H., Walhout, E. Q., and O'Brien, R. E.: Fresh versus Photo-recalcitrant Secondary Organic Aerosol: Effects of Organic Mixtures on Aqueous Photodegradation of 4-Nitrophenol, Environ. Sci. Technol. Lett., 7, 248-253, 10.1021/acs.estlett.0c00177, 2020.
Chen, C., Han, Y., Guo, J., Zhou, L., and Lan, Y.: Assessing the role of silica gel in the degradation of p-nitrophenol via Zn(0)-activated persulfate, J Taiwan Inst Chem Eng, 88, 169-176, https://doi.org/10.1016/j.jtice.2018.03.053, 2018.
355 Claeys, M., Vermeylen, R., Yasmeen, F., Gómez-González, Y., Chi, X., Maenhaut, W., Mészáros, T., and Salma, I.: Chemical characterisation of humic-like substances from urban, rural and tropical biomass burning environments using liquid chromatography with UV/vis photodiode array detection and electrospray ionisation mass spectrometry, Environ. Chem., 9, 273-284, https://doi.org/10.1071/EN11163, 2012.
Cordell, R. L., Mazet, M., Dechoux, C., Hama, S. M. L., Staelens, J., Hofman, J., Stroobants, C., Roekens, E., Kos, G. P. A.,
360 Weijers, E. P., Frumau, K. F. A., Panteliadis, P., Delaunay, T., Wyche, K. P., and Monks, P. S.: Evaluation of biomass burning across North West Europe and its impact on air quality, Atmos. Environ., 141, 276-286, https://doi.org/10.1016/j.atmosenv.2016.06.065, 2016.
Daneshvar, N., Behnajady, M. A., and Zorriyeh Asghar, Y.: Photooxidative degradation of 4-nitrophenol (4-NP) in UV/H_2O_2 process: Influence of operational parameters and reaction mechanism, J. Hazard. Mater., 139, 275-279,
365 https://doi.org/10.1016/j.jhazmat.2006.06.045, 2007.
Desyaterik, Y., Sun, Y., Shen, X., Lee, T., Wang, X., Wang, T., and Collett Jr., J. L.: Speciation of "brown" carbon in cloud water impacted by agricultural biomass burning in eastern China, J. Geophys. Res. Atmos., 118, 7389-7399, https://doi.org/10.1002/jgrd.50561, 2013.

Di Paola, A., Augugliaro, V., Palmisano, L., Pantaleo, G., and Savinov, E.: Heterogeneous photocatalytic degradation of nitrophenols, J. Photochem. Photobiol. A: Chem., 155, 207-214, https://doi.org/10.1016/S1010-6030(02)00390-8, 2003.

Ding, R., Mao, Z.-Y., and Wang, J.-L.: Synergistic effects of 4-nitrophenol degradation using gamma irradiation combined with a advanced oxidation process, Nucl. Sci. Tech., 27, 4, 10.1007/s41365-016-0004-y, 2016.

Du, J., Che, D., Li, X., Guo, W., and Ren, N.: Factors affecting p-nitrophenol removal by microscale zero-valent iron coupling with weak magnetic field (WMF), RSC Adv., 7, 18231-18237, 10.1039/C7RA02002C, 2017.

Feng, Y., Ramanathan, V., and Kotamarthi, V. R.: Brown carbon: a significant atmospheric absorber of solar radiation?, Atmos. Chem. Phys., 13, 8607-8621, 10.5194/acp-13-8607-2013, 2013.

Fleming, L. T., Lin, P., Roberts, J. M., Selimovic, V., Yokelson, R., Laskin, J., Laskin, A., and Nizkorodov, S. A.: Molecular composition and photochemical lifetimes of brown carbon chromophores in biomass burning organic aerosol, Atmos. Chem. Phys., 20, 1105-1129, 10.5194/acp-20-1105-2020, 2020.

Forrister, H., Liu, J., Scheuer, E., Dibb, J., Ziemba, L., Thornhill, K. L., Anderson, B., Diskin, G., Perring, A. E., Schwarz, J. P., Campuzano-Jost, P., Day, D. A., Palm, B. B., Jimenez, J. L., Nenes, A., and Weber, R. J.: Evolution of brown carbon in wildfire plumes, Geophys. Res. Lett., 42, 4623-4630, https://doi.org/10.1002/2015GL063897, 2015.

Frka, S., Šala, M., Kroflič, A., Huš, M., Čusak, A., and Grgić, I.: Quantum Chemical Calculations Resolved Identification of Methylnitrocatechols in Atmospheric Aerosols, Environ. Sci. Technol., 50, 5526-5535, 10.1021/acs.est.6b00823, 2016.

García Einschlag, F. S., Carlos, L., and Capparelli, A. L.: Competition kinetics using the UV/H_2O_2 process: a structure reactivity correlation for the rate constants of hydroxyl radicals toward nitroaromatic compounds, Chemosphere, 53, 1-7, https://doi.org/10.1016/S0045-6535(03)00388-6, 2003.

Gierczak, T., Bernard, F., Papanastasiou, D. K., and Burkholder, J. B.: Atmospheric Chemistry of c-C_5HF_7 and c-C_5F_8: Temperature-Dependent OH Reaction Rate Coefficients, Degradation Products, Infrared Spectra, and Global Warming Potentials, J. Phys. Chem., 125, 1050-1061, 10.1021/acs.jpca.0c10561, 2021.

Gonzalez, M. G., Oliveros, E., Wörner, M., and Braun, A. M.: Vacuum-ultraviolet photolysis of aqueous reaction systems, J. Photochem. Photobiol. C: Photochem. Rev., 5, 225-246, https://doi.org/10.1016/j.jphotochemrev.2004.10.002, 2004.

Harrison, M. A. J., Heal, M. R., and Cape, J. N.: Evaluation of the pathways of tropospheric nitrophenol formation from benzene and phenol using a multiphase model, Atmos. Chem. Phys., 5, 1679-1695, 10.5194/acp-5-1679-2005, 2005a.

Harrison, M. A. J., Barra, S., Borghesi, D., Vione, D., Arsene, C., and Iulian Olariu, R.: Nitrated phenols in the atmosphere: a review, Atmos. Environ., 39, 231-248, https://doi.org/10.1016/j.atmosenv.2004.09.044, 2005b.

Heal, M. R., Harrison, M. A. J., and Neil Cape, J.: Aqueous-phase nitration of phenol by N_2O_5 and $ClNO_2$, Atmos. Environ., 41, 3515-3520, https://doi.org/10.1016/j.atmosenv.2007.02.003, 2007.

Hems, R. F. and Abbatt, J. P. D.: Aqueous Phase Photo-oxidation of Brown Carbon Nitrophenols: Reaction Kinetics, Mechanism, and Evolution of Light Absorption, ACS Earth Space Chem., 2, 225-234, 10.1021/acsearthspacechem.7b00123, 2018.

Hems, R. F., Schnitzler, E. G., Liu-Kang, C., Cappa, C. D., and Abbatt, J. P. D.: Aging of Atmospheric Brown Carbon Aerosol, ACS Earth Space Chem., 5, 722-748, 10.1021/acsearthspacechem.0c00346, 2021.

Hems, R. F., Schnitzler, E. G., Bastawrous, M., Soong, R., Simpson, A. J., and Abbatt, J. P. D.: Aqueous Photoreactions of Wood Smoke Brown Carbon, ACS Earth Space Chem., 4, 1149-1160, 10.1021/acsearthspacechem.0c00117, 2020.

Herrmann, H., Hoffmann, D., Schaefer, T., Bräuer, P., and Tilgner, A.: Tropospheric Aqueous-Phase Free-Radical Chemistry: Radical Sources, Spectra, Reaction Kinetics and Prediction Tools, ChemPhysChem, 11, 3796-3822, https://doi.org/10.1002/cphc.201000533, 2010.

Herrmann, H., Schaefer, T., Tilgner, A., Styler, S. A., Weller, C., Teich, M., and Otto, T.: Tropospheric Aqueous-Phase Chemistry: Kinetics, Mechanisms, and Its Coupling to a Changing Gas Phase, Chem. Rev., 115, 4259-4334, 10.1021/cr500447k, 2015.

Hettiyadura, A. P. S., Garcia, V., Li, C., West, C. P., Tomlin, J., He, Q., Rudich, Y., and Laskin, A.: Chemical Composition and Molecular-Specific Optical Properties of Atmospheric Brown Carbon Associated with Biomass Burning, Environ. Sci. Technol., 55, 2511-2521, 10.1021/acs.est.0c05883, 2021.

Inomata, S., Fushimi, A., Sato, K., Fujitani, Y., and Yamada, H.: 4-Nitrophenol, 1-nitropyrene, and 9-nitroanthracene emissions in exhaust particles from diesel vehicles with different exhaust gas treatments, Atmos. Environ., 110, 93-102, https://doi.org/10.1016/j.atmosenv.2015.03.043, 2015.

Jaber, F., Schummer, C., Al Chami, J., Mirabel, P., and Millet, M.: Solid-phase microextraction and gas chromatography–mass spectrometry for analysis of phenols and nitrophenols in rainwater, as their t-butyldimethylsilyl derivatives, Anal.
420 Bioanal. Chem., 387, 2527-2535, 10.1007/s00216-006-1115-9, 2007.

Jacobson, M. Z.: Isolating nitrated and aromatic aerosols and nitrated aromatic gases as sources of ultraviolet light absorption, J. Geophys. Res. Atmos., 104, 3527-3542, https://doi.org/10.1029/1998JD100054, 1999.

Jiang, H., Frie, A. L., Lavi, A., Chen, J. Y., Zhang, H., Bahreini, R., and Lin, Y.-H.: Brown Carbon Formation from Nighttime Chemistry of Unsaturated Heterocyclic Volatile Organic Compounds, Environ. Sci. Technol. Lett., 6, 184-190,
425 10.1021/acs.estlett.9b00017, 2019.

Jiang, W., Misovich, M. V., Hettiyadura, A. P. S., Laskin, A., McFall, A. S., Anastasio, C., and Zhang, Q.: Photosensitized Reactions of a Phenolic Carbonyl from Wood Combustion in the Aqueous Phase—Chemical Evolution and Light Absorption Properties of AqSOA, Environ. Sci. Technol., 10.1021/acs.est.0c07581, 2021.

Kahnt, A., Behrouzi, S., Vermeylen, R., Safi Shalamzari, M., Vercauteren, J., Roekens, E., Claeys, M., and Maenhaut, W.:
430 One-year study of nitro-organic compounds and their relation to wood burning in PM10 aerosol from a rural site in Belgium, Atmos. Environ., 81, 561-568, https://doi.org/10.1016/j.atmosenv.2013.09.041, 2013.

Kavitha, V. and Palanivelu, K.: Degradation of nitrophenols by Fenton and photo-Fenton processes, J. Photochem. Photobiol. A: Chem., 170, 83-95, https://doi.org/10.1016/j.jphotochem.2004.08.003, 2005.

Kitanovski, Z., Grgić, I., Vermeylen, R., Claeys, M., and Maenhaut, W.: Liquid chromatography tandem mass spectrometry
435 method for characterization of monoaromatic nitro-compounds in atmospheric particulate matter, J. Chromatogr. A, 1268, 35-43, https://doi.org/10.1016/j.chroma.2012.10.021, 2012.

Kitanovski, Z., Shahpoury, P., Samara, C., Voliotis, A., and Lammel, G.: Composition and mass size distribution of nitrated and oxygenated aromatic compounds in ambient particulate matter from southern and central Europe – implications for the origin, Atmos. Chem. Phys., 20, 2471-2487, 10.5194/acp-20-2471-2020, 2020.

440 Kotronarou, A., Mills, G., and Hoffmann, M. R.: Ultrasonic irradiation of p-nitrophenol in aqueous solution, J. Phys. Chem., 95, 3630-3638, 10.1021/j100162a037, 1991.

Laskin, A., Laskin, J., and Nizkorodov, S. A.: Chemistry of Atmospheric Brown Carbon, Chem. Rev., 115, 4335-4382, 10.1021/cr5006167, 2015.

Lemaire, J., Guth, J. A., Klais, O., Leahey, J., Merz, W., Philp, J., Wilmes, R., and Wolff, C. J. M.: Ring test of a method for
445 assessing the phototransformation of chemicals in water, Chemosphere, 14, 53-77, https://doi.org/10.1016/0045-6535(85)90041-4, 1985.

Li, C., He, Q., Hettiyadura, A. P. S., Käfer, U., Shmul, G., Meidan, D., Zimmermann, R., Brown, S. S., George, C., Laskin, A., and Rudich, Y.: Formation of Secondary Brown Carbon in Biomass Burning Aerosol Proxies through NO_3 Radical Reactions, Environ. Sci. Technol., 54, 1395-1405, 10.1021/acs.est.9b05641, 2020.

450 Liang, Y., Wang, X., Dong, S., Liu, Z., Mu, J., Lu, C., Zhang, J., Li, M., Xue, L., and Wang, W.: Size distributions of nitrated phenols in winter at a coastal site in north China and the impacts from primary sources and secondary formation, Chemosphere, 250, 126256, https://doi.org/10.1016/j.chemosphere.2020.126256, 2020.

Lipczynska-Kochany, E.: Novel method for a photocatalytic degradation of 4-nitrophenol in homogeneous aqeuous solution, Environ. Technol., 12, 87-92, 10.1080/09593339109384985, 1991.

455 Liu, Y., Wang, D., Sun, B., and Zhu, X.: Aqueous 4-nitrophenol decomposition and hydrogen peroxide formation induced by contact glow discharge electrolysis, J. Hazard. Mater., 181, 1010-1015, https://doi.org/10.1016/j.jhazmat.2010.05.115, 2010.

Lu, Z., Streets, D. G., Winijkul, E., Yan, F., Chen, Y., Bond, T. C., Feng, Y., Dubey, M. K., Liu, S., Pinto, J. P., and Carmichael, G. R.: Light Absorption Properties and Radiative Effects of Primary Organic Aerosol Emissions, Environ. Sci.
460 Technol., 49, 4868-4877, 10.1021/acs.est.5b00211, 2015.

Majewska, M., Khan, F., Pieta, I. S., Wróblewska, A., Szmigielski, R., and Pieta, P.: Toxicity of selected airborne nitrophenols on eukaryotic cell membrane models, Chemosphere, 266, 128996, https://doi.org/10.1016/j.chemosphere.2020.128996, 2021.

Mohr, C., Lopez-Hilfiker, F. D., Zotter, P., Prévôt, A. S. H., Xu, L., Ng, N. L., Herndon, S. C., Williams, L. R., Franklin, J.
465 P., Zahniser, M. S., Worsnop, D. R., Knighton, W. B., Aiken, A. C., Gorkowski, K. J., Dubey, M. K., Allan, J. D., and Thornton, J. A.: Contribution of Nitrated Phenols to Wood Burning Brown Carbon Light Absorption in Detling, United Kingdom during Winter Time, Environ. Sci. Technol., 47, 6316-6324, 10.1021/es400683v, 2013.

Moise, T., Flores, J. M., and Rudich, Y.: Optical Properties of Secondary Organic Aerosols and Their Changes by Chemical Processes, Chem. Rev., 115, 4400-4439, 10.1021/cr5005259, 2015.

470 Natangelo, M., Mangiapan, S., Bagnati, R., Benfenati, E., and Fanelli, R.: Increased concentrations of nitrophenols in leaves from a damaged forestal site, Chemosphere, 38, 1495-1503, https://doi.org/10.1016/S0045-6535(98)00370-1, 1999.

NCAR TUV calculator: https://www.acom.ucar.edu/Models/TUV/Interactive_TUV/, last access: Sep 2021.

Niessen, R., Lenoir, D., and Boule, P.: Phototransformation of phenol induced by excitation of nitrate ions, Chemosphere, 17, 1977-1984, https://doi.org/10.1016/0045-6535(88)90009-4, 1988.

475 O'Neill, P., Steenken, S., van der Linde, H., and Schulte-Frohlinde, D.: Reaction of OH radicals with nitrophenols in aqueous solution, Radiat. Phys. Chem., 12, 13-17, https://doi.org/10.1016/0146-5724(78)90070-5, 1978.

Oturan, M. A., Peiroten, J., Chartrin, P., and Acher, A. J.: Complete Destruction of p-Nitrophenol in Aqueous Medium by Electro-Fenton Method, Environ. Sci. Technol., 34, 3474-3479, 10.1021/es990901b, 2000.

Randolph, C., Lahive, C. W., Sami, S., Havenith, R. W. A., Heeres, H. J., and Deuss, P. J.: Biobased Chemicals: 1,2,4-
480 Benzenetriol, Selective Deuteration and Dimerization to Bifunctional Aromatic Compounds, Org Process Res Dev, 22, 1663-1671, 10.1021/acs.oprd.8b00303, 2018.

Rapf, R. J., Dooley, M. R., Kappes, K., Perkins, R. J., and Vaida, V.: pH Dependence of the Aqueous Photochemistry of α-Keto Acids, J. Phys. Chem., 121, 8368-8379, 10.1021/acs.jpca.7b08192, 2017.

Regueiro, J., Becerril, E., Garcia-Jares, C., and Llompart, M.: Trace analysis of parabens, triclosan and related chlorophenols
485 in water by headspace solid-phase microextraction with in situ derivatization and gas chromatography–tandem mass spectrometry, J. Chromatogr. A, 1216, 4693-4702, https://doi.org/10.1016/j.chroma.2009.04.025, 2009.

Rived, F., Rosés, M., and Bosch, E.: Dissociation constants of neutral and charged acids in methyl alcohol. The acid strength resolution, Anal. Chim. Acta, 374, 309-324, https://doi.org/10.1016/S0003-2670(98)00418-8, 1998.

Sander, R.: Compilation of Henry's law constants (version 4.0) for water as solvent, Atmos. Chem. Phys., 15, 4399-4981,
490 10.5194/acp-15-4399-2015, 2015.

Sobczyński, A., Duczmal, Ł., and Zmudziński, W.: Phenol destruction by photocatalysis on TiO2: an attempt to solve the reaction mechanism, J Mol Catal A Chem, 213, 225-230, https://doi.org/10.1016/j.molcata.2003.12.006, 2004.

Tan, Y., Perri, M. J., Seitzinger, S. P., and Turpin, B. J.: Effects of Precursor Concentration and Acidic Sulfate in Aqueous Glyoxal−OH Radical Oxidation and Implications for Secondary Organic Aerosol, Environ. Sci. Technol., 43, 8105-8112,
495 10.1021/es901742f, 2009.

Tauber, A., Schuchmann, H.-P., and von Sonntag, C.: Sonolysis of aqueous 4-nitrophenol at low and high pH, Ultrason Sonochem, 7, 45-52, https://doi.org/10.1016/S1350-4177(99)00018-8, 2000.

TenBrook, P. L., Kendall, S. M., Viant, M. R., and Tjeerdema, R. S.: Toxicokinetics and biotransformation of p-nitrophenol in red abalone (Haliotis rufescens), Aquat. Toxicol., 62, 329-336, https://doi.org/10.1016/S0166-445X(02)00103-0, 2003.

500 Tilgner, A., Schaefer, T., Alexander, B., Barth, M., Collett Jr, J. L., Fahey, K. M., Nenes, A., Pye, H. O. T., Herrmann, H., and McNeill, V. F.: Acidity and the multiphase chemistry of atmospheric aqueous particles and clouds, Atmos. Chem. Phys., 21, 13483-13536, 10.5194/acp-21-13483-2021, 2021.

Vidović, K., Kroflič, A., Šala, M., and Grgić, I.: Aqueous-Phase Brown Carbon Formation from Aromatic Precursors under Sunlight Conditions, Atmosphere, 11, 131, 2020.

505 Vione, D., Maurino, V., Minero, C., and Pelizzetti, E.: Aqueous Atmospheric Chemistry: Formation of 2,4-Dinitrophenol upon Nitration of 2-Nitrophenol and 4-Nitrophenol in Solution, Environ. Sci. Technol., 39, 7921-7931, 10.1021/es050824m, 2005.

Vione, D., Maurino, V., Minero, C., Borghesi, D., Lucchiari, M., and Pelizzetti, E.: New Processes in the Environmental Chemistry of Nitrite. 2. The Role of Hydrogen Peroxide, Environ. Sci. Technol., 37, 4635-4641, 10.1021/es0300259, 2003.

510 Vione, D., Maurino, V., Minero, C., Duncianu, M., Olariu, R.-I., Arsene, C., Sarakha, M., and Mailhot, G.: Assessing the transformation kinetics of 2- and 4-nitrophenol in the atmospheric aqueous phase. Implications for the distribution of both nitroisomers in the atmosphere, Atmos. Environ., 43, 2321-2327, https://doi.org/10.1016/j.atmosenv.2009.01.025, 2009.

Wang, X., Heald, C. L., Ridley, D. A., Schwarz, J. P., Spackman, J. R., Perring, A. E., Coe, H., Liu, D., and Clarke, A. D.: Exploiting simultaneous observational constraints on mass and absorption to estimate the global direct radiative forcing of
515 black carbon and brown carbon, Atmos. Chem. Phys., 14, 10989-11010, 10.5194/acp-14-10989-2014, 2014.

Witkowski, B., Al-sharafi, M., and Gierczak, T.: Kinetics and products of the aqueous-phase oxidation of β-caryophyllonic acid by hydroxyl radicals, Atmos. Environ., 213, 231-238, https://doi.org/10.1016/j.atmosenv.2019.06.016, 2019.

Wojnárovits, L. and Takács, E.: Irradiation treatment of azo dye containing wastewater: An overview, Radiat. Phys. Chem., 77, 225-244, https://doi.org/10.1016/j.radphyschem.2007.05.003, 2008.

520 Xie, M., Chen, X., Hays, M. D., and Holder, A. L.: Composition and light absorption of N-containing aromatic compounds in organic aerosols from laboratory biomass burning, Atmos. Chem. Phys., 19, 2899-2915, 10.5194/acp-19-2899-2019, 2019.

Xiong, X., Sun, Y., Sun, B., Song, W., Sun, J., Gao, N., Qiao, J., and Guan, X.: Enhancement of the advanced Fenton process by weak magnetic field for the degradation of 4-nitrophenol, RSC Adv., 5, 13357-13365, 10.1039/C4RA16318D,
525 2015.

Yan, J., Wang, X., Gong, P., Wang, C., and Cong, Z.: Review of brown carbon aerosols: Recent progress and perspectives, Sci. Total Environ., 634, 1475-1485, https://doi.org/10.1016/j.scitotenv.2018.04.083, 2018.

Zhang, W., Xiao, X., An, T., Song, Z., Fu, J., Sheng, G., and Cui, M.: Kinetics, degradation pathway and reaction mechanism of advanced oxidation of 4-nitrophenol in water by a UV/H_2O_2 process, J. Chem. Technol. Biotechnol, 78, 788-
530 794, https://doi.org/10.1002/jctb.864, 2003.

Zhang, Y., Forrister, H., Liu, J., Dibb, J., Anderson, B., Schwarz, J. P., Perring, A. E., Jimenez, J. L., Campuzano-Jost, P., Wang, Y., Nenes, A., and Weber, R. J.: Top-of-atmosphere radiative forcing affected by brown carbon in the upper troposphere, Nat. Geosci., 10, 486-489, 10.1038/ngeo2960, 2017.

Zhao, R., Lee, A. K. Y., Huang, L., Li, X., Yang, F., and Abbatt, J. P. D.: Photochemical processing of aqueous atmospheric
535 brown carbon, Atmos. Chem. Phys., 15, 6087-6100, 10.5194/acp-15-6087-2015, 2015.

Zhao, S., Ma, H., Wang, M., Cao, C., and Yao, S.: Study on the role of hydroperoxyl radical in degradation of p-nitrophenol attacked by hydroxyl radical using photolytical technique, J. Photochem. Photobiol. A: Chem., 259, 17-24, https://doi.org/10.1016/j.jphotochem.2013.02.012, 2013.